

A LASER-BASED EXPLOSIVES SENSOR

Rosario C. Sausa
U.S. Army Research Laboratory
AMSRD-ARL-WM-BD
Aberdeen Proving Ground, MD 21005-5066

Jerry Cabalo
US Army Edgewood Chemical Biological Center
Edgewood, MD 21010

ABSTRACT

Trace explosives residues of CL20 (hexanitrohexazaisowurtzitane) and RDX (hexahydro-1,3,5-hexanitro-1,3,5-triazine) are measured in real-time by surface laser photofragmentation-fragment detection (SPF-FD) spectroscopy at ambient conditions. A 248-nm laser photofragments the target residue on a substrate, and a 226-nm laser ionizes the resulting NO fragment by resonance-enhanced multiphoton ionization by means of its A-X (0,0) transitions near 226 nm. We investigate the effects of laser wavelength and energy, delay between photofragmentation and ionization lasers, and residue concentration on signal intensity. A signal-to-noise analysis yields a limit of detection of 7.1 ng/cm² for CL20 and 1.4 ng/cm² for RDX at 1atm and 298K.

1. INTRODUCTION

The sensitive detection of explosive compounds in real time at ambient pressure and temperature is a key issue for detecting potential terrorist operations and aviation security. Two laser spectroscopic techniques for detecting TNT (2,4,6 trinitrotoluene) in the gas phase are cavity ring down spectroscopy (CRDS) (Usachev et al., 2001 and Todd et al., 2002) and laser photofragmentation (PF) - fragment detection (FD) spectroscopy (Swayambunathan et al., 1999, Boudreaux et al., 1999, Swayambunathan et al., 2000, Arusi-Parpar et al., 2001, and Heflinger et al., 2002). The CRDS technique probes the parent molecule, whereas the PF-FD technique probes the characteristic NO photofragment by laser-induced fluorescence (LIF) or resonance-enhanced multiphoton ionization (REMPI). The NO fragment is characteristic of the NO₂

functional group that is present in these molecules. Both techniques can detect TNT in the ppm/v-ppb/v range near ambient conditions. However, these techniques cannot detect other important energetic materials such as CL20 and RDX at ambient conditions because their vapor pressure concentration is several of magnitudes less than that of TNT at 298K and 1 atm.

Laser irradiation of the solid energetic materials with ultraviolet (uv) light is a means of generating gaseous molecules or fragments that can be detected by mass spectrometry, optical spectroscopy, or both. Photochemical and photothermal processes produce atomic and molecular fragments from the surface. Tang and coworkers show that the 226-nm irradiation of RDX produces both positive and negative ion masses ranging from 15 to 176 amu (Tang et al. 1987). They assign the m/z=30 peak to NO. Dickinson and coworkers observe small masses of both neutral and ionic species, including NO, as well as photoelectrons when they irradiate RDX crystals with 248-nm light at a fluence < 5 mJ/cm² (Dickinson et al., 1990).

In this paper, we report the detection of CL20 and RDX residues *in situ* and in real time by surface laser photofragmentation-fragment detection (SPF-FD) at ambient conditions. A low power laser operating in the ultraviolet photofragments the target molecule on a surface and a second low power laser tuned to 226 nm ionizes the characteristic NO fragment by REMPI using its A-X (0,0) transitions. An ion probe with miniature, square electrodes collects the resulting electrons and ions. We report the limits of detection (LOD) at ambient conditions, and present a detailed study of the issues influencing sensitivity.

Report Documentation Page

*Form Approved
OMB No. 0704-0188*

Public reporting burden for the collection of information is estimated to average 1 hour per response, including the time for reviewing instructions, searching existing data sources, gathering and maintaining the data needed, and completing and reviewing the collection of information. Send comments regarding this burden estimate or any other aspect of this collection of information, including suggestions for reducing this burden, to Washington Headquarters Services, Directorate for Information Operations and Reports, 1215 Jefferson Davis Highway, Suite 1204, Arlington VA 22202-4302. Respondents should be aware that notwithstanding any other provision of law, no person shall be subject to a penalty for failing to comply with a collection of information if it does not display a currently valid OMB control number.

1. REPORT DATE 01 NOV 2006	2. REPORT TYPE N/A	3. DATES COVERED -	
4. TITLE AND SUBTITLE A Laser-Based Explosives Sensor		5a. CONTRACT NUMBER	
		5b. GRANT NUMBER	
		5c. PROGRAM ELEMENT NUMBER	
6. AUTHOR(S)		5d. PROJECT NUMBER	
		5e. TASK NUMBER	
		5f. WORK UNIT NUMBER	
7. PERFORMING ORGANIZATION NAME(S) AND ADDRESS(ES) U.S. Army Research Laboratory AMSRD-ARL-WM-BD Aberdeen Proving Ground, MD 21005-5066		8. PERFORMING ORGANIZATION REPORT NUMBER	
9. SPONSORING/MONITORING AGENCY NAME(S) AND ADDRESS(ES)		10. SPONSOR/MONITOR'S ACRONYM(S)	
		11. SPONSOR/MONITOR'S REPORT NUMBER(S)	
12. DISTRIBUTION/AVAILABILITY STATEMENT Approved for public release, distribution unlimited			
13. SUPPLEMENTARY NOTES See also ADM002075., The original document contains color images.			
14. ABSTRACT			
15. SUBJECT TERMS			
16. SECURITY CLASSIFICATION OF:			17. LIMITATION OF ABSTRACT
a. REPORT unclassified	b. ABSTRACT unclassified	c. THIS PAGE unclassified	UU
			18. NUMBER OF PAGES 5
			19a. NAME OF RESPONSIBLE PERSON

2. APPARATUS

Figure 1 is a schematic of the experimental apparatus. The details of the apparatus and SPF-FD technique are described in detail in our previous publication (Cabalo and Sausa, 2005). Solid CL20 films are prepared by spreading drops of CL20 in acetone solutions on a glass slide substrate and then evaporating the acetone. The slide is positioned horizontally and moved by an XYZ micrometer stage to refresh the film sampled.

The REMPI probe consists of two 15-mm x 15-mm metal plates with 2-mm holes for the passage of the excitation beam. The separation of the plates is 6 mm. The probe is placed parallel to the substrate with the lower, insulated plate positioned about ~0.5 mm from the substrate surface. The probe is typically biased to 850 V, yielding an average field between the plates of ~140 V/mm.

SPF-FD utilizes both a pump laser and a probe laser. The pump beam is directed normal to the substrate surface, whereas the probe is directed between the plates, parallel to substrate surface, and intersects the probe beam at approximately 1 mm from the surface. Both beams are focused with a 10-cm lens. A 10-Hz, 5-ns Nd:YAG (Continuum Surelite III) laser generates the photolysis wavelengths of 355, 266, and 248 nm. Part of the infrared beam is frequency tripled for 355-nm photolysis, while the remainder pumps a dye laser (Lambda Physik, FL3002) whose output is frequency doubled for 248- or 266-nm photolysis. A second dye laser (Lumonics, HyperEx 300), pumped by a Nd:YAG (Continuum Surelite II) and whose output is frequency doubled, probes the NO fragment of the target molecule by (1+1) REMPI by means of its $A^2\Sigma^+ - X^2\Pi$ (0,0) transitions in the region of 226-227 nm. The laser energy for both pump and probe beams is in the range of 10-20 $\mu\text{J}/\text{pulse}$. A pulse generator (Stanford Research Systems, model DG 535) provides the delay between the photolysis and probe laser.

REMPI excitation spectra are recorded with 10-shot averaging at a fixed photolysis laser wavelength, while scanning the probe laser. The substrate is translated to replenish the film. Signal levels for the response plots are recorded

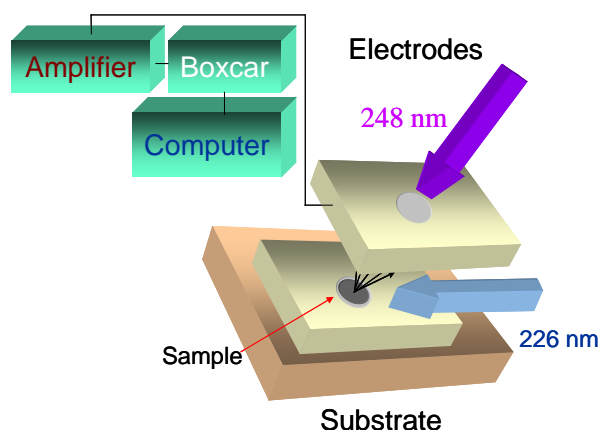


Fig. 1. Experimental apparatus

by scanning the substrate surface with the REMPI laser at a fixed wavelength of 226.18 nm and averaging the signal from a broad area of the substrate. This is done to mitigate the effect of the variation in film thickness across the substrate. A current amplifier (Keithley 427, gain $10^6 - 10^7$ V/A, time constant 0.01 ms) amplifies the electrode signal and a 125-MHz oscilloscope (Lecroy, 9400) monitors it. A personal computer records the signals from a boxcar averager (Stanford Research Systems, SR250).

A UV-visible spectrometer (Hewlett-Packard, Model 8453) with Hewlett-Packard Chemstation software records the absorbance spectra of RDX and CL20 in methanol or acetonitrile (2.25×10^{-5} M). The samples are more than 99% pure as determined by High Performance Liquid Chromatography.

3. RESULTS AND DISCUSSION

Figure 2 shows the experimental and calculated (1+1) REMPI spectra of NO from RDX in the region of 225.9–226.2 nm. The observed features are due to $A^2\Sigma^+ - X^2\Pi$ (0,0) transitions of NO. No REMPI signal is observed in the absence of either RDX film or photolysis laser light. A multi-parameter computer program based on a Boltzmann, rotational distribution analysis fits the observed data (Pastel and Sausa, 2000). Parameters include the laser line shape, temperature, and absolute and relative frequency values for the data. The program

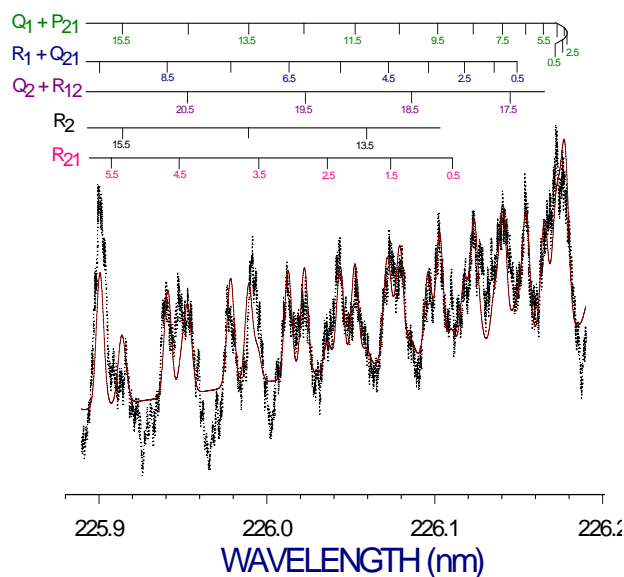


Fig. 2. Experimental (...) and calculated (-) spectra of NO from RDX.

utilizes the NO $A^2\Sigma^+ - X^2\Pi(0,0)$, one-photon line strengths and rotational energy levels calculated with ground and excited electronic spectroscopic constants for NO. The line strengths associated with the nonresonant, continuum transitions from the $A^2\Sigma^+$ state are assumed to be equal. Figure 2 shows that the calculated spectrum accounts for all the rotational lines of the Q_1 , P_{21} , R_1 , Q_{21} , Q_2 , R_{12} , R_2 , and R_{21} branches of NO, and fits the observed data rather well. The best fit to the observed data using a Gaussian function for the laser line shape yields a temperature of $325\text{K} \pm 25\text{K}$, indicating that the NO fragment is nearly thermally equilibrated in the timescale and pressure of the experiment. A similar analysis of a REMPI spectrum of NO (3 ppm) recorded at room temperature and 1 atm yields a temperature of $310\text{K} \pm 10\text{K}$.

The sensitivity of the SPF-FD technique depends in part on the laser photolysis wavelength. Figure 3 shows the NO REMPI signals from RDX for common laser photolysis wavelengths in the ultraviolet, 248, 266, and 355 nm. The signal increases with decreasing wavelength. At 248 nm the signal is approximately a factor two greater than at 266 nm, and at 355 nm little, if any, signal is observed. Figure 3 also shows the molar absorptivities of RDX at the respective photolysis wavelengths for comparison purposes. The SPF-FD signal levels scale roughly with the molar absorptivities, indicating that the amount of NO produced from RDX is in

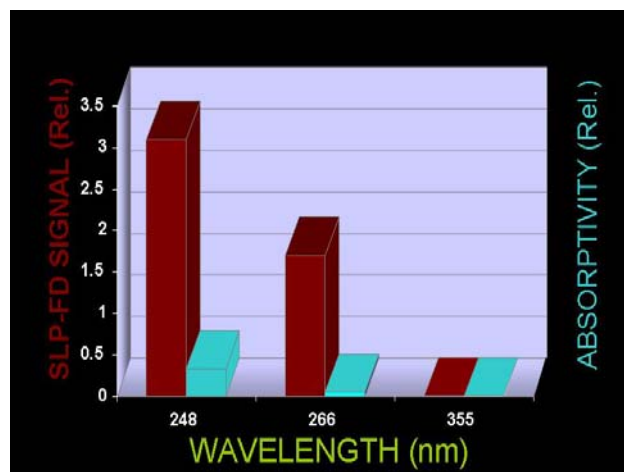


Fig. 3. Dependence of signal intensity on photolysis wavelength and RDX absorptivity.

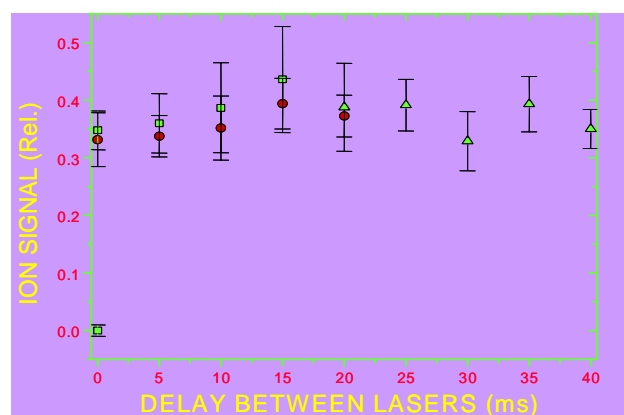


Fig. 4. Signal intensity as a function of pump and probe delay.

part a function of the absorption coefficient of RDX at the selected photolysis wavelength.

Figure 4 shows the signal of NO from RDX as a function of delay between photolysis and ionization lasers. All delay times between 0.1 and 40 ms result in the same signal indicating that the NO concentration from RDX reaches a steady state value very quickly. Our studies also show that the SPF-FD signal increases linearly with photolysis laser energy up to $12\ \mu\text{J}$, and then begins to level off. A delay of 1 ms and a photolysis laser energy of $15\ \mu\text{J}$ is arbitrarily selected for further study.

Figure 5 shows the response curves of RDX and CL20. The signal levels are measured using the SPF-FD technique with both photolysis and probe lasers set at a fixed wavelength ($\lambda_1 =$

248 nm and $\lambda_2 = 226.18$ nm). The limits of detection are defined by $3\sigma/R$, where R is the signal response and σ is the root mean square of the noise. The best fit of the data yields an LOD of 1.4 ng/cm² for RDX and 7.1 ng/cm² for CL20. If all of the RDX molecules irradiated by the pump laser are converted to NO, and the NO molecules expand uniformly filling a hemisphere, then the probe laser samples $\sim 3.3 \times 10^7$ molecules of NO (~ 400 pg of RDX). This value compares favorably to the 200-pg value obtained by Raman Microscopy by Chang and coworkers (Cheng et al., 1995).

The sensitivity of the SPF-FD technique for each energetic material depends on the amount of NO produced at 248 nm, and the amount of NO detected at 226.18 nm. In our LOD measurements, the probe energy and optical setup are the same for both compounds; thus, the amount of NO produced at 248 nm depends on the absorption coefficient of the target compound at 248 nm and the governing mechanism that produces NO. The 248-nm extinction coefficients of RDX and CL20 are 7.6×10^3 and 1.5×10^4 , respectively. Thus, *a priori*, we expect the LOD of CL20 to be about twice that of RDX. Instead, we observe that the LOD of CL20 is about five times that of RDX. Clearly, the mechanism for NO production also contributes to the sensitivity of the SPF-FD technique.

RDX has a ring structure and contains three nitro functional groups ($-\text{NO}_2$), whereas CL20 has a cage structure and contains six nitro functional groups. In both molecules the nitro functional group is bonded to a nitrogen atom, which is bonded to the rest of the molecule by a carbon atom, $\text{C}-\text{N}-\text{NO}_2$. The mechanisms involved in the 248-nm laser-irradiation of RDX and CL20 are complex. They may include photothermal and photochemical processes, as well as surface effects. Among the many initial steps suggested in the condensed-phase decomposition of these molecules, the most likely step is the homolysis of one their nitro functional groups, which is weakly bound to the rest of the molecule. NO_2 may then react further to produce NO. The $\text{N}-\text{NO}_2$ bond dissociation energy of RDX and CL20 are similar, around 34 to 39 kcal/mol (Wu and Fried, 1997, Kuklja and Kunz, 2001, and Rice, 2004). However, CL20 has an LOD that is a factor of nearly 5 times greater than that of RDX. This suggests that the process of NO_2 release in these molecules is

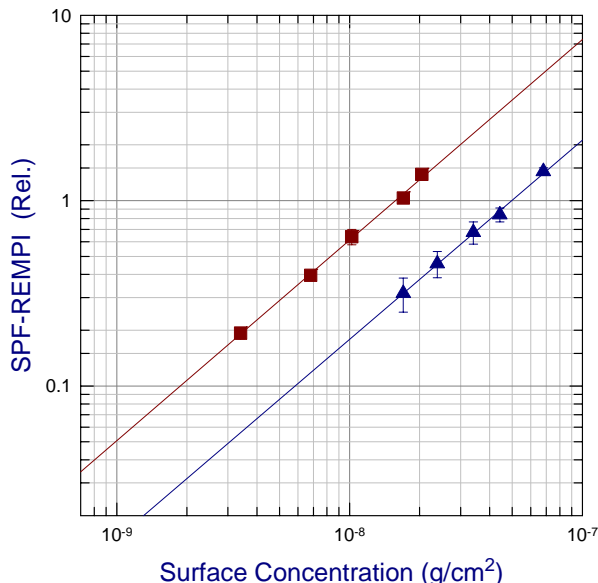


Fig. 5. RDX and CL20 response plots

more complicated than the simple cleavage of a single nitro functional group and may involve the loss of more than one nitro group from each molecule. In the case of RDX, the energy for the ring's $\text{C}-\text{N}$ bond cleavage is lowered after NO_2 homolysis because the ring structure makes it sterically difficult for the radical site to stabilize itself by interacting with its other parts. As a result, the radical can decompose further and liberate additional NO_2 (Patil and Brill, 1991). In contrast, in CL20 the energy of its $\text{C}-\text{N}$ bond is raised following NO_2 homolysis because its cage structure promotes the stabilization of the radical site by rearrangement or multiple bond formation with other parts of the backbone. (Patil and Brill, 1991, and Geetha et al., 2003). This stabilization hinders additional NO_2 loss. Thus, the LOD of CL20 is greater than that of RDX because it releases less NO_2 in its decomposition than RDX. Although our argument for CL20's LOD being larger than that of RDX is plausible, other governing processes may be operable.

3. CONCLUSION

We have detected residues of CL20 and RDX on surfaces by SLP-FD. The technique uses an ultraviolet laser to photolyze the target molecule and a second 226-nm laser to ionize the resulting NO photofragment by REMPI. The technique's sensitivity depends on photolysis wavelength. Maximum signal is observed at 248 nm, over 266 and 355 nm, where the absorption

coefficient of the target molecule is the strongest. A detection threshold of 1.4 ng/cm² for RDX and 7.1 ng/cm² for is determined at 1 atm and room temperature with 10-20 μJ of photolysis and probe laser energy. SPF-FD is a gentle technique that relies on low power UV photolysis instead of heating of the target surface, thus permitting the analysis of delicate substrate materials.

ACKNOWLEDGEMENTS

We thank Dr. B. Rice of the US Army Research Laboratory (ARL) for calculating the N-NO₂ bond energy in CL20, Drs. R. Pesce-Rodriguez and P. Kaste of ARL for the energetic material samples, and Drs. A. Kotlar and M. Schroeder of ARL for many helpful discussions.

REFERENCES

- Arusi-Parpar, T., Heflinger, D. and Lavi, R., 2001: Photodissociation Followed by Laser-Induced Fluorescence at Atmospheric Pressure and 24 Degrees C: A Unique Scheme for Remote Detection of TNT, *Applied Optics* **40** (36), 6677-6681.
- Boudreaux, G., Miller, T., Kunecke, A., Singh, J., Yueh, F., Monts, D., 1999: "Development of a photofragmentation laser-induced-fluorescence laser sensor for detection of 2,4,6-trinitrotoluene in soil and groundwater, *Appl. Opt.* **38**(9), 1411-1417.
- Cabalo, J. Sausa, R., 2005: Trace Detection of Explosives with Low Vapor Pressure Emissions by Laser Surface Photofragmentation-Fragment Detection Spectroscopy Using an Improved Ionization Probe," *Applied Optics*, **44**(6), 1084-1091, and reference therein.
- Cheng, C., Kirkbridge, T.E., Batchelder, D.N., Lacey, R.J. and Sheldon, T.G., 1995: In-Situ Detection and Identification of Trace Explosives by Raman Microscopy," *Journal of Forensic Sciences* **40**, 31-37.
- Dickinson, J., Jensen, L., Doering, D., and Lee, R., 1990: Mass-spectroscopy study of products from exposure of cyclotrimethylene-trinitramine single-crystals to KrF excimer laser-radiation, *J. Appl. Phys.* **67** (8), 3641-3651.
- Geetha, M., Nair, U.R., Sarwade, D.B., Gore, G.M., Asthana, S.N. and Singh, H., 2003: Studies on CL20: The Most Powerful High Energy Material," *Journal of Thermal Analysis and Calorimetry* **73**, 913-922.
- Heflinger, D., Arusi-Parpar, T., Ron, Y., and Lavi, R., 2002: Application of a unique scheme for remote detection of explosives," *Optics Communications* **204** (1-6), 327-331.
- Kuklja, M.M. and Kunz, A.B., 2001: Electronic Structure of Molecular Crystals Containing Edge Dislocations," *Journal of Applied Physics* **89** (9), 4962-4970.
- Pastel, R.L. Sausa, R.C., 2000: Spectral Differentiation of Trace Concentrations of NO₂ from NO by Laser Photofragmentation with Fragment Ionization at 226 and 452 nm: Quantitative Analysis of NO-NO₂ Mixtures," *Applied Optics* **39**(15), 2487-2495.
- Patil, D.G. and Brill, T.B., 1991: Thermal Decomposition of Energetic Materials 53. Kinetics and Mechanisms of Thermolysis of Hexanitrohexazaisowurtzitane," *Combustion and Flame* **87**, 145-151.
- Rice, B., 2004: US Army Research Laboratory, private communication. A preliminary density functional theory calculation at the B3LYP/6-31G* level yields a CL20 N-NO₂ bond strength of 38.6 kcal/mol. The error limit is ± a few kca//mol.
- Swayambunathan, V., Singh, G. Sausa, R., 1999: Laser Photofragmentation-Fragment Detection and Pyrolysis-Laser-Induced Fluorescence Studies on Energetic Materials, *Appl. Optics* **38**(30), 6447-6454..
- Swayambunathan, V., Singh, G. Sausa, R., 2000: Investigations into trace detection of nitrocompounds by one- and two-color laser photofragmentation/fragment detection spectrometry," *Appl. Spectrosc.* **54**(5), 651-658.
- Tang, T., Chaudhri, M., Rees, C., Mullock, S., 1987: Decomposition of solid explosives by laser irradiation-a mass-spectrometric study, *J. Mater. Sci.* **22** (3), 1037-1044.
- Usachev, A., Miller, T., Singh, J., Yueh, F., Jang, P. and Monts, D., 2001: *Applied Spectroscopy*, **55**(2), 125-131.
- Wu, C.J. and Fried, L.E., 1977: Ab Initio Study of RDX Decomposition Mechanisms," *J. Phys. Chem. A* **101**, 8675-8679.